Colloid & Polymer Science Colloid Polym Sci 272:1474–1485 (1994)

Phase separation of symmetric polymer mixtures in a common good solvent in the semidilute concentration regime*)

A Sariban[1]) and K. Binder

Institut für Physik, Johannes Gutenberg-Universität Mainz, FRG
[1]) *Present Address*: Institute für Physikalische Chemie, Technische Hochschule Darmstadt, Darmstadt, FRG

*) *Dedicated to Prof. Fischer on the occasion of his 65th birthday.*
Both of the authors are deeply indebted to Prof. E.W. Fischer, not only for help, support, and enlightening discussions, but even for bringing them together and suggesting to them to collaborate! By this "catalytic" action he actually played a decisive role in creating a longstanding and successful collaboration, the latest results of which are presented below.

Abstract: Monte Carlo simulations of lattice models of binary (AB) symmetric polymer mixtures (chain lengths $N_A = N_B = N$) in a common good solvent are carried out and the phase diagrams and critical properties of the unmixing transitions are estimated and interpreted in terms of recent theories. Polymers are modeled by self-avoiding walks of length $N = 16$, 32 and 64 on the simple cubic lattice. Data for vacancy concentrations of $\phi_V = 0.6$, 0.8 and 0.85 are analyzed. It is shown that for $N = 16$, $\phi_V = 0.85$ no phase separation occurs, down to the lowest temperature, while for $N = 32$, $\phi_V = 0.85$ still phase separation occurs but no longer is complete. Our results are compatible with a scaling theory based on a "renormalization" of the Flory–Huggins χ-parameter due to "blob" effects.

Keywords: Polymer mixtures – Monte Carlo simulation – critical phenomena – Flory–Huggins parameter – semidilute solutions

1. Introduction

Understanding the compatibility or incompatibility of polymer blends has become a very active area of research recently [1–22]. Much of this discussion is devoted to better understanding the molecular origin of the Flory–Huggins χ-parameter [23–25] and, in particular, its entropic contributions in dense polymer melts [9–11, 13–15]. Here we focus on another entropic effect that comes into play when one considers polymer mixtures in the presence of a solvent [16–22]: assuming that the solvent is a good solvent for both types of polymers A,B, one must expect that in the semidilute [26] concentration regime excluded volume interactions play a decisive role on all length scales smaller than a blob size [26, 27] (see Fig. 1). Each blob typically contains monomers of a single coil only, and since unmixing only is caused by (short range) interactions between monomers belonging to different chains [8, 28], it follows that the number of such contacts is anomalously reduced due to blob formation. Although the chains in the semidilute concentration regime (defined by requiring for the volume fraction ϕ taken by the monomers via the inequality $\phi^* \ll \phi \ll 1$, where ϕ^* is the volume fraction of chain overlap) are still strongly interpenetrating, they become more and more compatible because now, locally, they don't "see" each other, and the excluded volume interaction prevents most of these binary short range forces between different types of monomers to contribute.

The Flory–Huggins theory [23] in its simplest form would predict that diluting a symmetrical binary polymer blend (chain lengths

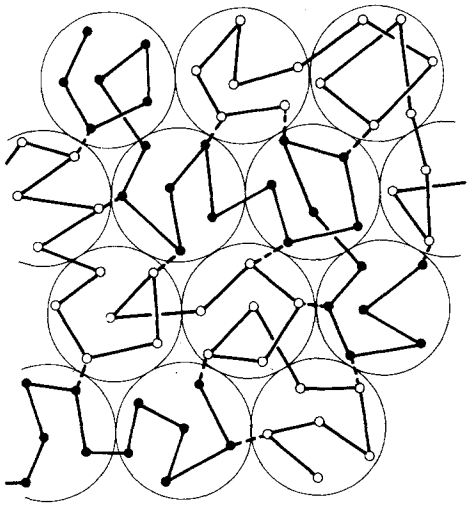

Fig. 1. Blob picture of a binary polymer blend (A, B) in a common good solvent. Two types of monomers are indicated by open and full dots, respectively. Each chain can be decomposed into a chain of "blobs" of radius r_b containing n_b monomers, such that $r_b \propto n_b^{\upsilon}$ where the exponent $\upsilon \approx 0.59$ [26] characterizes coil linear dimensions in a good solvent. For simplicity it is assumed that the solvent quality is the same for both polymers, in the sense that they have the same blob radius (shown by circles). Binary short-range interactions (ε_{AB}) between different kinds of monomers (shown as broken straight lines) can occur only between monomers which are both in the surface region of different blobs

$N_A = N_B = N$) decreases the critical temperature T_c of unmixing simply proportional to the volume fraction ϕ of the monomers [7, 8, 29]

$$k_B T_c/\varepsilon_{AB} = \frac{1}{2} z N \phi \tag{1}$$

Here, it is assumed, as is standard [23] that the polymers are represented by self- and mutually avoiding random walks on a lattice of coordination number z, and the only interaction considered apart from excluded volume is a repulsive energy ε_{AB} between monomers of different kind at nearest neighbor sites. Equation (1) implies that irrespective how small ϕ is, there always should be a critical temperature of unmixing, even in the dilute regime.

In the theories taking excluded volume effects into account [16–22], one finds that there is a new exponent x that describes the effective renormalization of the effective χ parameter as $\phi \to 0$,

$$\chi_{\text{eff}} \propto \frac{\varepsilon_{AB}}{k_B T} \phi^{x/(3\upsilon-1)}, \quad x \approx 0.22 . \tag{2}$$

The mean-field critical condition is then that $\chi_{\text{eff}}^{\text{crit}} \tilde{N} = 2$, with $\tilde{N} = N/n_b$ being the number of monomers per blob. Using the condition that the blob radius r_b scales as $r_b \sim n_b^{\upsilon}$, $\upsilon \approx 0.59$ [26], and that in the semidilute regime each monomer is part of a blob, one concludes $\phi r_b^3 = n_b$ since the system is homogeneous, omitting all prefactors of order unity, and thus $n_b \propto \phi^{-1/(3\upsilon-1)}$. Thus, the scaling theories [16–22] predict instead of Eq. (1) a more complicated dependence of the critical temperature on chain length and volume fraction ϕ,

$$\frac{\varepsilon_{AB}}{k_B T_c} \phi^{x/(3\upsilon-1)} \propto \tilde{N}^{-1} \propto (N\phi^{-1/(3\upsilon-1)})^{-1}, \quad \text{for } \tilde{N} \gg 1 . \tag{3}$$

In addition, no unmixing can occur when ϕ falls far below ϕ^* (which can be defined by $\tilde{N} = 1$), and, hence, one finds that the critical temperature falls to zero already at a characteristic volume fraction ϕ^{comp} (of the same order as ϕ^*) below which the mixture is strictly compatible, irrespective of the value of $\varepsilon_{AB}/k_B T$.

While some experiments exist [30–33] that are possibly qualitatively compatible with these predictions, a quantitative test of Eq. (3) does not exist, however: real mixtures neither are precisely symmetric, nor are real solvents of exactly the same quality for both polymers, and for a quantitative interpretation of the experimental data all these asymmetries hence must be accounted for. Also often a rather narrow temperature range is usually at the disposal only – limited at low temperatures by the glass transition, at high temperatures by chemical degradation of the polymers or evaporation of the solvent – and thus decisive experiments are very difficult.

All these difficulties are eliminated when considering computer experiments on simple model systems, of course. The aim of the present work hence is to test Eq. (3) and to show that for small enough $\tilde{N}$ phase separation does not occur at all. Section 2 very briefly describes the model and simulation technique. Section 3 describes our data for $\phi = 0.15$, where both a case will be analyzed ($N = 16$) where no transition occurs at all, and a case ($N = 64$) where the behavior is exactly equivalent to the higher volume fractions studied previously [7, 8, 28]. The case $N = 32$ is a borderline situation, where still a transition occurs, but not all chains take part in it. Section 4 discusses

then the scaling behavior of critical amplitudes with chain lengths in the semidilute regime [34], while Section 5 summarizes our conclusions.

2. Model and simulation technique

As in our previous work [7, 8, 28], we use $L \times L \times L$ simple cubic lattices with periodic boundary conditions at a fixed vacancy concentration $\phi_V = 1 - \phi$ of vacant sites, and the remaining sites are taken by monomers of the two types of polymers, which are represented as self- and mutually avoiding walks of $(N - 1)$ links on the lattice (Fig. 2). Chain lengths $N = 16$ are studied for lattice sizes in the range $L = 20, 24, 30$, $N = 32$ in the range $L = 24, 30, 40$, and $N = 64$ in the range $L = 30, 40, 50$. These linear dimensions are sufficient, since even for the smallest ϕ studied here ($\phi = 0.15$) the (athermal) end-to-end distance of the chains is still distinctly smaller than $L/2$ $\{\langle R^2 \rangle^{1/2} = 5.14$ for $N = 16$; 7.84 for $N = 32$; and 11.7 for $N = 64$, respectively$\}$. Also the number of chains with these sizes is still large enough (for $\phi = 0.15$ $N_{\text{chains}} = 75 - 253$ for $N = 16$; $65 - 300$ for $N = 32$; $63 - 293$ for $N = 64$) to allow probing of collective phenomena. Of course, the number of chains has always to be integer and this means that for some choices of L the volume fraction deviates slightly from 0.15, but we consider the error that this deviation introduces to be insignificant.

As in our previous work, starting configurations were grown by inversely restricted sampling [35, 36] and then carefully equilibrated in the athermal limit ($\varepsilon_{AB}/k_B T = 0$) where both chains are identical. For an estimation of the overlap concentration ϕ^*, a crossover scaling analysis of the linear dimensions in the athermal case was performed (Fig. 3). Despite the shortness of our

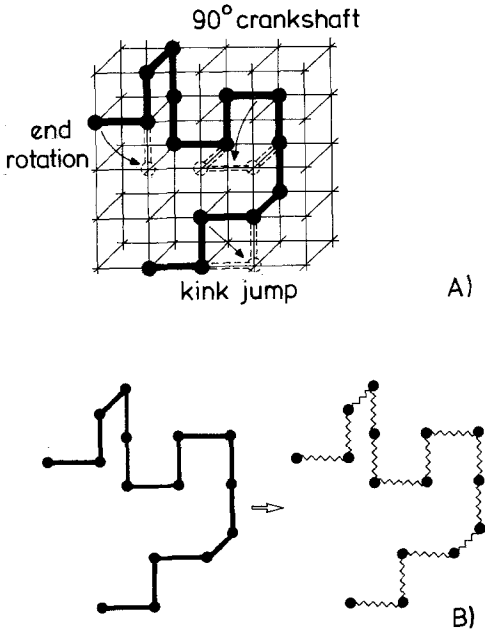

Fig. 2. Moves used to equilibrate polymer coil configurations for the self-avoiding walk model on the simple cubic lattice (upper part): end rotations, kink jump motions, and crank-shaft rotations. From time to time these local moves alternate with a semi-grandcanonical move (lower part) where one attempts to replace an A-chain by a B-chain in an identical coil configuration, or vice versa. In the transition probability of this move, both the chemical potential difference $\Delta\mu$ as well as the energy change $\delta\mathscr{H}$ enter

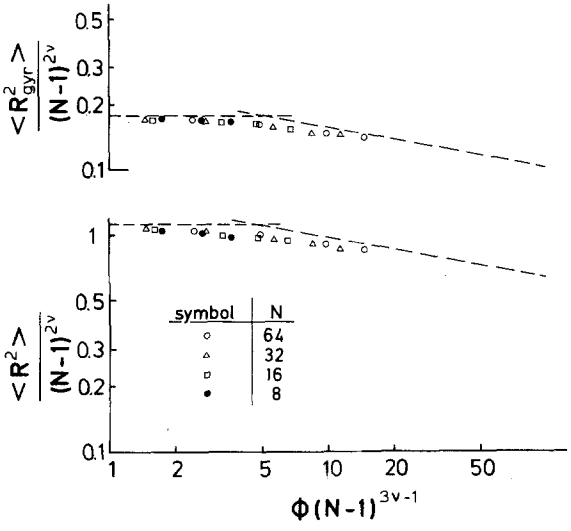

Fig. 3. Log-log plot of the mean square gyration radius $\langle R^2_{gyr} \rangle$ normalized by the asymptotic chain length dependence $(N - 1)^{2\upsilon}$, $\upsilon = 0.59$, (upper part) and of the normalized mean square end-to-end distance (lower part) versus the crossover scaling variable $\phi(N - 1)^{3\upsilon - 1}$. Data for chain lengths $N = 8$ to $N = 64$ are included. Since these chains are rather short, it is necessary to express the power laws in terms of the number of links $(N - 1)$ rather than the number of monomers (N), since then corrections to scaling are smaller. The horizontal dashed straight line indicates the single-chain behavior studied separately, while the other straight line illustrates the slope that results in the regime of semidilute concentrations $\{\langle R^2_{gyr} \rangle \propto \langle R^2 \rangle \propto \phi^{-(3\upsilon-1)/(2\upsilon-1)} N\}$

chains, the data are compatible with the expected crossover scaling behavior. Estimates for the dilute limit ($\phi \to 0$) were obtained independently as $\langle R^2 \rangle = 27.2$, $\langle R^2_{gyr} \rangle = 4.39$ ($N = 16$); $\langle R^2 \rangle = 65$, $\langle R^2_{gyr} \rangle = 10.3$ ($N = 32$); and $\langle R^2 \rangle = 148$, $\langle R^2_{gyr} \rangle = 23.7$ ($N = 64$), respectively. From Fig. 3 it is suggestive to estimate the overlap concentration ϕ^* from the point, where deviations from the dilute behavior start to become appreciable, e.g., for $\phi^*(N-1)^{3\nu-1} \approx 3$. This criterion would yield $\phi^*(N = 64) \approx 0.123$. The alternative definition requiring that the gyration volumina of the chains in the dilute regime provides a dense filling of space,

$$N/\{4\pi\langle R^2_{gyr}\rangle^{3/2}/3\} = \phi^* , \tag{4}$$

yields $\phi^*(N = 16) \approx 0.415$, $\phi^*(N = 32) \approx 0.23$ and $\phi^*(N = 64) \approx 0.132$. Both methods of estimating ϕ^* signifies no sharp boundary but rather a smooth crossover only. These estimates also show that our volume fractions $\phi = 0.15$, 0.20, and 0.40 are almost always in a regime where ϕ and ϕ^* are comparable. For the short chains studied here, ϕ^* is so large that the condition for the semidilute regime has to be relaxed to $\phi^* \lesssim \phi < 1$ (the stricter condition $\phi^* \ll \phi \ll 1$ could only be satisfied for much longer chains, of course). Only for the case $N = 16$, $\phi = 0.15$ do we have a clearcut dilute situation, and thus a different behavior in this situation is readily expected.

Due to the strict symmetry between A and B in our model, we know that phase coexistence can occur only for chemical potential difference $\Delta\mu = \mu_A - \mu_B = 0$. Thus a single parameter $\varepsilon_{AB}/k_B T$ needs to be varied to locate the critical temperature of our model for each choice of para-

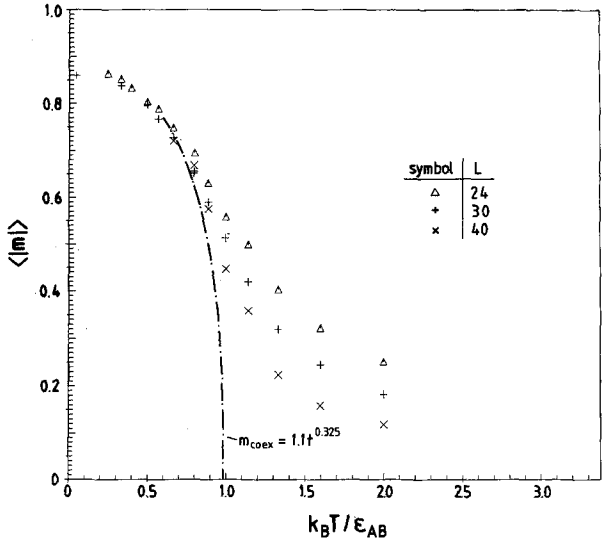

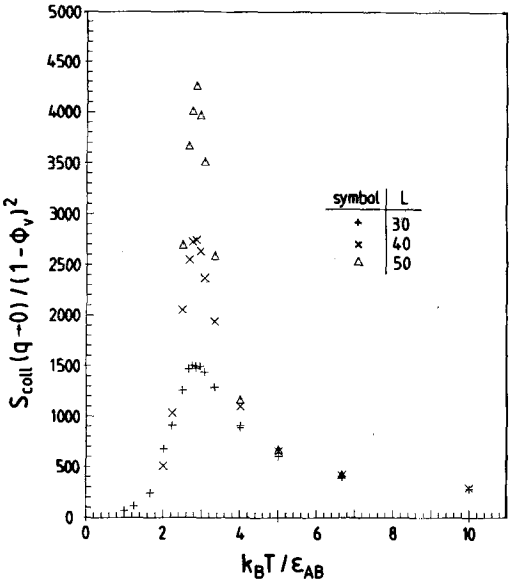

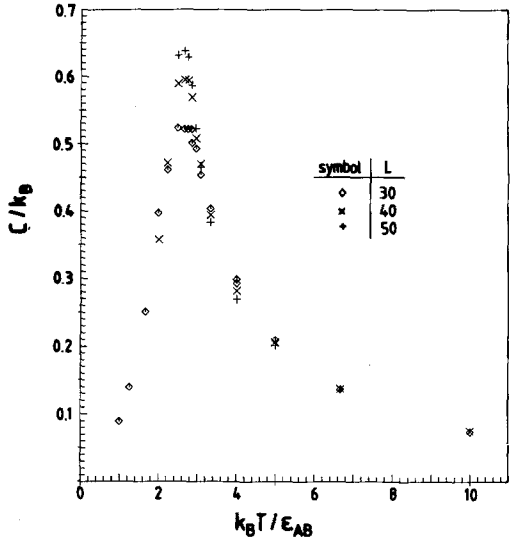

Fig. 4. a) Absolute value of the order parameter $\langle |m| \rangle$ of the unmixing transition {Eq. (5)} plotted vs. temperature $k_B T/\varepsilon_{AB}$ for the case $N = 64$, $\phi_V = 0.85$, and three linear dimensions. Dash-dotted curve shows the coexistence curve m_{coex} extracted from the finite size scaling analysis. Critical temperature is estimated from cumulant intersections (Fig. 5a) as $k_B T_c/\varepsilon_{AB} = 2.83 \pm 0.02$.
b) Normalized scattering function $S_{coll}(q \to 0)/(1 - \phi_v)^2$ for the case $N = 64$, $\phi_v = 0.85$ plotted vs. temperature $k_B T/\varepsilon_{AB}$. Arrow shows $k_B T_c/\varepsilon_{AB}$.
c) Specific heat per chain plotted vs. temperature for the case $N = 64$, $\phi_V = 0.85$. Arrow shows $k_B T_c/\varepsilon_{AB}$

meters $\{\phi_V, N\}$. As in our previous work [7, 8, 28] we find it convenient to work in the semigrand-canonical ensemble, where from time to time chains are considered for a switch of their identity from A to B or vice versa at otherwise fixed configuration. The volume fractions of A-monomers ϕ_A, ϕ_B are then fluctuating variables and are obtained from a sampling of the numbers $\mathcal{N}_A$, $\mathcal{N}_B$ of A-chains (B-chains) in the system or the associated order parameter $\langle|m|\rangle$

$$m = (\mathcal{N}_A - \mathcal{N}_B)/(\mathcal{N}_A + \mathcal{N}_B)\,,$$
$$\phi_A = (1 - \phi_v)(1 + m)/2\,, \qquad (5)$$
$$\phi_B = (1 - \phi_v)(1 - m)/2$$

In the disordered phase, we have $\langle\phi_A\rangle = \langle\phi_B\rangle = (1 - \phi_v)/2$ for $\Delta\mu = 0$, and hence there $\langle|m|\rangle_L \to 0$ for $L \to \infty$, while in the ordered phase $\langle|m|\rangle_L \to m_{coex}$ describing the two coexisting A-rich and B-rich phases,

$$\phi^{(1)}_{A,coex} = \frac{1}{2}(1 - \phi_v)(1 + m_{coex}) = \phi^{(2)}_{B,coex}\,, \qquad (6)$$

$$\phi^{(2)}_{A,coex} = \frac{1}{2}(1 - \phi_v)(1 - m_{coex}) = \phi^{(1)}_{B,coex}\,. \qquad (7)$$

Equations (6, 7) exhibit the symmetry of interchanging A↔B in our model, which simply means a sign change of the order parameter. Figure 4 shows that indeed the expected behavior occurs for $\phi_v = 0.85$, $N = 64$: $\langle|m|\rangle \to 1$ for $T \to 0$ means that the phase separation between A and B is complete.

Quantities useful to locate the phase transition are also the response function $S_{coll}(q \to 0)$ which measures the scattering intensity due to concentration fluctuations in the long wavelength limit ($\vec{q}$ = scattering wavevector), which from the simulation is obtained via a fluctuation relation

$$S_{coll}(q \to 0) = (\mathcal{N}_A + \mathcal{N}_B)N(1 - \phi_v) \times [\langle m^2\rangle - \langle|m|\rangle^2]\,. \qquad (8)$$

This quantity for $T \to T_c$ shows a critical divergence, which for a finite lattice is rounded off, of course (Fig. 4b). Also, the singularity in the specific heat (which follows from energy fluctuations) is rounded, Fig. 4c, and hence for an accurate estimation of T_c and of the coexistence curve a finite scaling analysis is required. This is discussed in the next section. Here, we simply emphasize that the data in Fig. 4 are qualitatively very similar to those of our previous work [7, 8, 28], where volume fractions up to $\phi = 0.8$ ($\phi_v = 0.2$) were used. As discussed above, $\phi = 0.15$ for $N = 64$ exceeds the overlap concentration ϕ^* only slightly but nevertheless the unmixing transition still occurs in full analogy to concentrated solutions [7, 8, 28] and melts [37].

3. Monte Carlo results for symmetric blends near the overlap threshold ϕ^*

The theory of finite size scaling near critical points [38] implies

$$\langle|m|^k\rangle = L^{-k\beta/\upsilon}\tilde{f}_k(L^{1/\upsilon_t}t), \quad t = 1 - T/T_c\,, \qquad (9)$$

where β is the critical exponent of the order parameter $\{m_{coex} = \hat{B}(1 - T/T_c)^\beta\}$, υ_t the critical exponent of the correlation length $\{\xi = \hat{\xi}_\pm|1 - T/T_c|^{-\upsilon_t}$, the $\pm$ signs refer to temperatures above (+) and below (−)$T_c\}$, and $\tilde{f}_k$ is a scaling function. From Eq. (9) it is easy to show that for normalized ratios such as the fourth-order cumulant the power law prefactors $L^{-k\beta/\upsilon_t}$ cancel out,

$$U_L \equiv 1 - \langle m^4\rangle/[3\langle m^2\rangle^2] = \tilde{U}(L^{1/\upsilon_t}t)\,, \qquad (10)$$

with another scaling function $\tilde{U} \equiv 1 - \tilde{f}_4/3\tilde{f}_2^2$. From Eq. (10) it follows that different curves U_L vs t must intersect in a common intersection point $\tilde{U}(0)$ at $t = 0$ ($T = T_c$), irrespective of L. Locating such a cumulant intersection hence is an unbiased method to find T_c, if there is a critical point at all. Figure 5 shows that we can locate a critical point for $\phi = 0.15$ both for $N = 64$ and for $N = 32$ but not for $N = 16$. It is seen that for $N = 16$ the cumulants increase as ε_{AB}/k_BT increases but for $\varepsilon_{AB}/k_BT \approx 3$ the increase stops and the data for large L fall systematically below the data for smaller L. This is an indication that for $N = 16$ one stays in the disordered phase throughout, down to the lowest temperatures. Also the data for the specific heat (Fig. 6a) and scattering function (Fig. 6b) are consistent with this interpretation: the specific heat only shows a broad Schottky-like anomaly, and there is hardly any size effect visible, rather distinct from the data of Fig. 4b. Also the scattering function does not show a peak down to the lowest temperatures studied, but rather a pronounced increase to

rather large values. The drastic size effects at very low temperatures indicate the presence of large clusters of A-chains and large clusters of B-chains, which are of the order of the linear dimensions of our lattices studied. Of course, for $N = 16$, $\phi = 0.15$ is distinctly below ϕ^*, $\phi \approx 0.40^*$, and thus no "spanning cluster" of macroscopic size of chains still interacting with each other is then expected, as will be discussed in Section 5.

Under these circumstances it should not be a surprise that the case $\phi = 0.15$, $N = 32$ (where already $\phi \approx \frac{2}{3}\phi^*$, see estimates above) behaves in

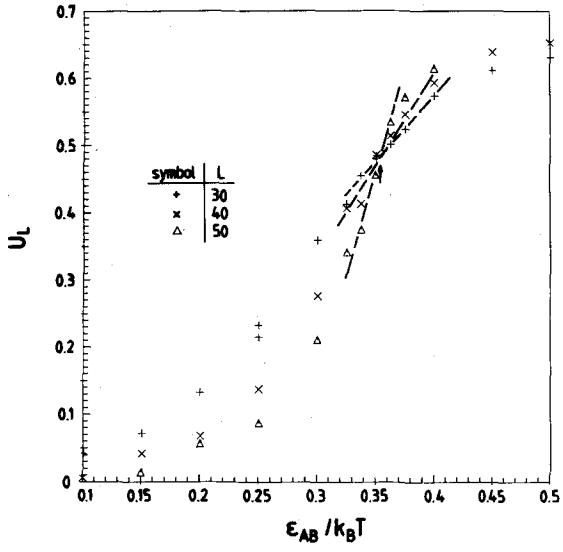

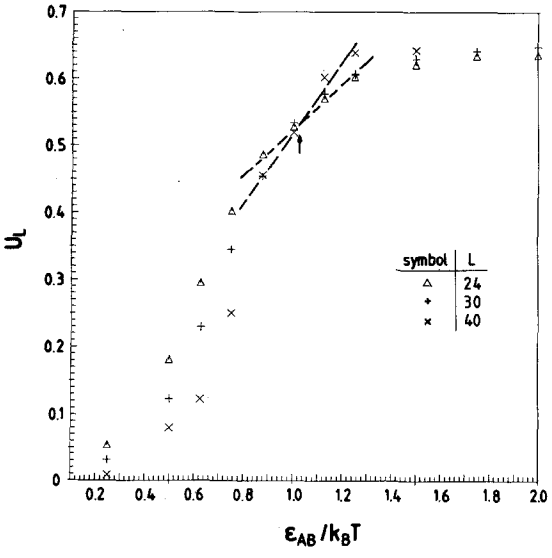

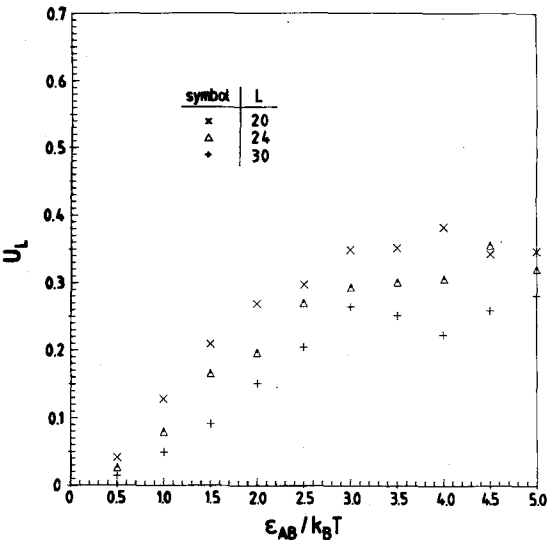

Fig. 5. Cumulant U_L plotted vs. $\varepsilon_{AB}/k_B T$ for $\phi = 0.15$ and $N = 64$(a), $N = 32$(b) and $N = 16$(c). Arrow in cases a, b shows the estimated location of the critical point

an intermediate manner: the order parameter $\langle |m| \rangle$ does reach size-independent saturation values m_{coex} at low temperatures, but these saturation values do not go to complete phase separation $\{m_{coex}(T \to 0) \to 1$ is expected for $\phi > \phi^*\}$, but rather reach only a finite limit, $m_{coex}(T \to 0) \approx 0.87$ (Fig. 7a). This finding can again be interpreted in a kind of percolation-like language by stating that for ϕ slightly smaller than ϕ^* we have both a 'spanning cluster" of interacting coils (which "touch" each other at their outer surface regions and thus are able to transmit the effect of the repulsive interaction ε_{AB} between unlike monomers) and disconnected, smaller clusters of finite size, which do not contribute to the order parameter of the system. The fact that $N = 32$ must be close to a borderline case is also plausible from th specific heat (Fig. 7b) – which already is more similar to the Schottky peak (Fig. 6a) of the nonordering case ($N = 16$) rather than the critical divergence seen for $N = 64$ (Fig. 4c) – and the scattering function, Fig. 7c, which clearly shows a critical increase, but also some anomalously enhanced scattering intensity at low temperatures. Again, this excess scattering must be attributed to the disjoint clusters.

In cases where we have located a critical temperature, one may apply the finite size scaling

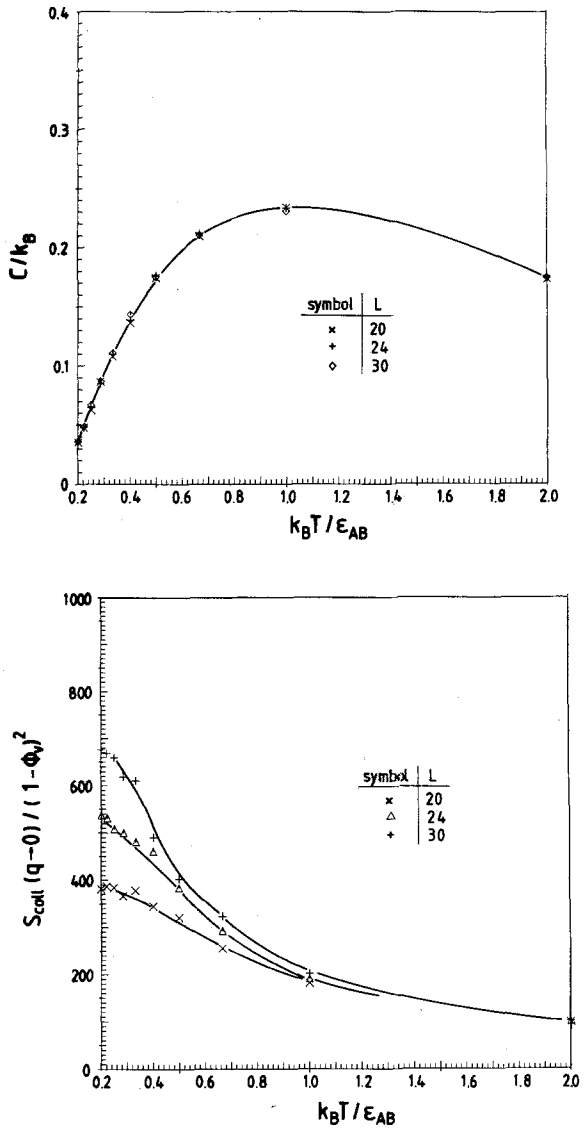

Fig. 6. Specific heat (a) and scattering functions (b) plotted vs. $k_B T/\varepsilon_{AB}$ for the case $N = 16$, $\phi_V = 0.85$, and three lattice linear dimensions as indicated. Curves are guides to the eye only

formula Eq.(9) by plotting $\langle|m|\rangle L^{\beta/\upsilon_I}$ versus L^{1/υ_I} t, using the critical exponent values of the Ising model universality class ($\beta \approx 0.325$, $\upsilon_I = 0.63$ [39]). Figure 8 shows that this works reasonably well, as for the higher volume fractions described earlier [7, 8, 28]. Since $\langle|m|\rangle L^{\beta/\upsilon_I} = \tilde{f}_1(tL^{\beta/\upsilon_I})$ must behave for large argument $\zeta = tL^{\beta/\upsilon_I}$ as $\tilde{f}_1(\zeta) = B\zeta^{\beta}$, in order that the correct thermodynamic limit results ($m_{coex} = \hat{B}t^{\beta}$), the straight lines on the log-log plots can be used to estimate the amplitude factors $\hat{B}$, and hence one can construct the coexistence curve near the critical temperature quantitatively. These results have been anticipated in Figs. 4a and 7a. Critical amplitudes for the scattering function can be inferred similarly, as described already in ref. [7].

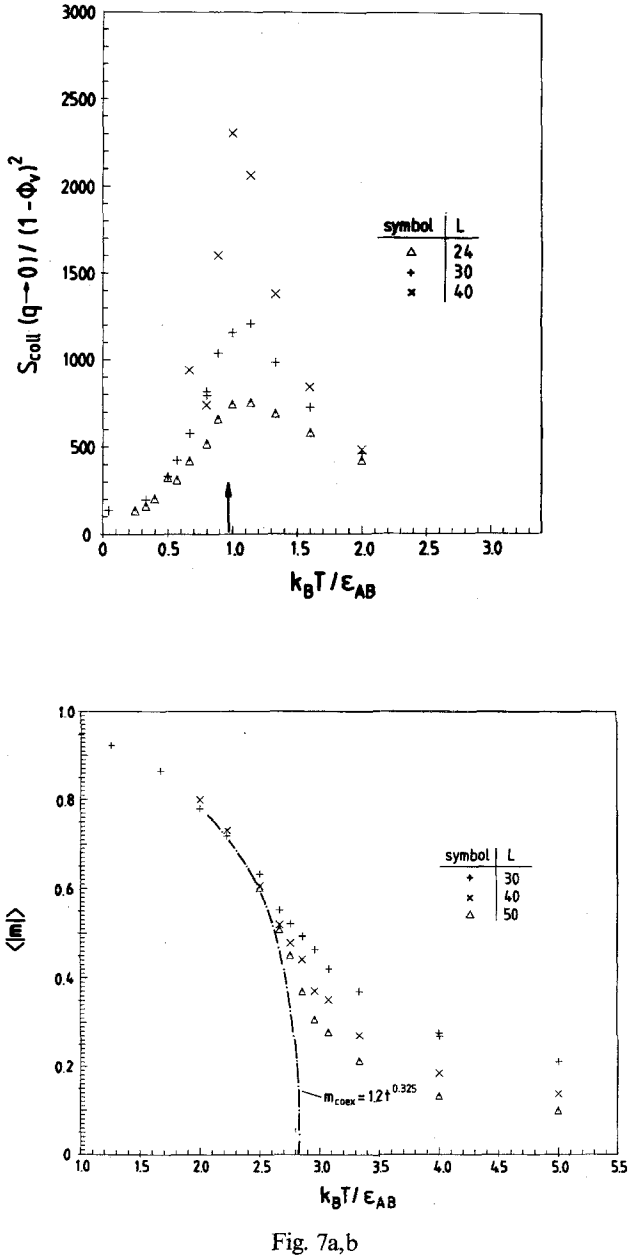

Fig. 7a,b

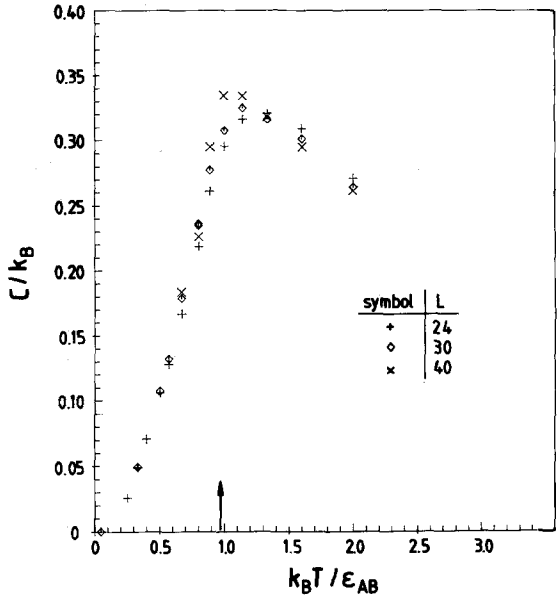

Fig. 7. Order parameter $\langle|m|\rangle$ (a), scattering function (b) and specific heat (c) plotted vs. temperature $k_B T_c/\varepsilon_{AB}$ for the case $N = 32$ and $\phi_V = 0.85$, Arrows show estimates for the critical temperature $k_B T_c/\varepsilon_{AB}$

Finally, the estimates for T_c for all values of ϕ and N can now be combined to test for Eq. (3). Figure 9 shows that for $N\phi^{1/(3\upsilon-1)} \gtrsim 4$, i.e., $\phi \gtrsim \phi^*$, this prediction is reasonably well fulfilled. Figure 9 thus is the central result of the present paper.

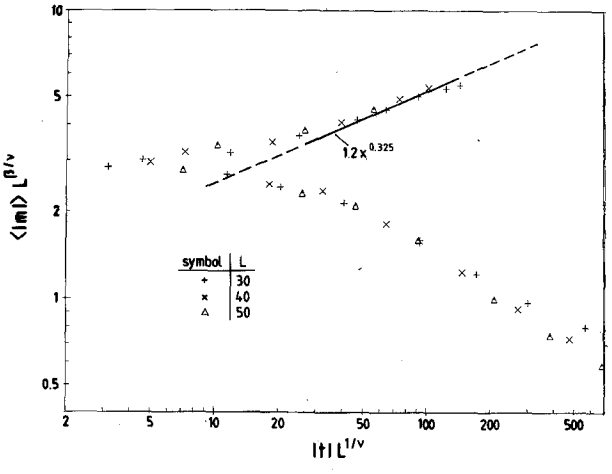

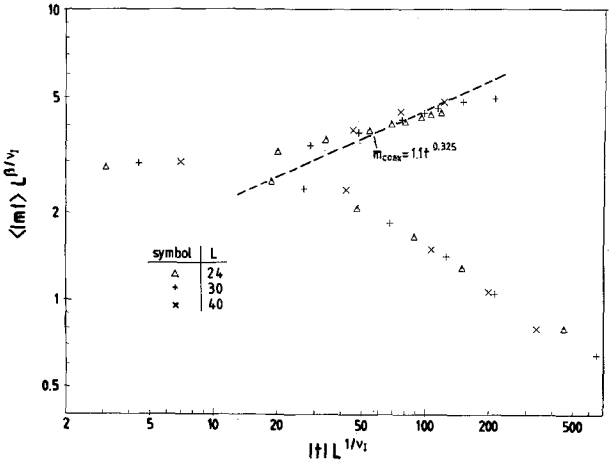

Fig. 8. Finite size scaling plots of the order parameter $\langle|m|\rangle L^{\beta/\upsilon_t}$ vs. $|t|L^{1/\upsilon_t}$ for the model with $\phi_V = 0.85$ and $N = 64$(a) and $N = 32$(b). Straight lines are the asymptotic relation $m_{coex} = \hat{B}t^{\beta}$ included in Figs. 4a and 7a, respectively. Here $k_B T_c/\varepsilon_{AB} = 0.98$ ($N = 32$) and 2.83 ($N = 64$) is used

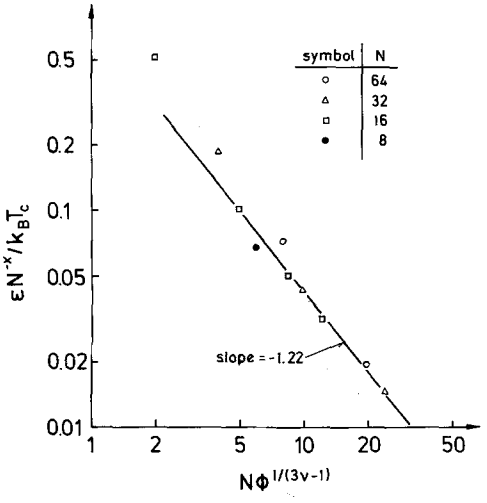

Fig. 9. Renormalized critical Flory–Huggins parameter $\varepsilon N^{-x}/k_B T_c$, with $x = 0.22$ [18] on a log-log plot vs. $N\phi^{1/(3\upsilon-1)}$ {this means a rescaling $\tilde{N} = N/n_b$ with the number of segments per blob, $n_b \propto \phi^{-1/(3\upsilon-1)}$, cf. Eq.(3).}. Straight line shows the asymptotic exponent of the scaling function $-(1 + x) = -1.22$

The increase of the data points for $\phi \lesssim \phi^*$ away from the straight line signifies that for $\phi < \phi^*$ one reaches a threshold value ϕ_{comp} where $\varepsilon/k_B T_c \to \infty$.

4. Critical amplitudes and crossover scaling near the overlap concentration ϕ^*

In dense polymer melts, the critical behavior of the unmixing transition is mean-field-like, apart from a narrow Ising-like critical region very close to T_c[1, 7, 26, 40–42]. This crossover is ruled by a "Ginzburg number" [43] Gi $\propto N^{-1}$, such that for $|t| \gg$ Gi the classical mean-field critical exponents $\beta_{MF} = 1/2$, $\upsilon_{MF} = 1/2$, $\gamma_{MF} = 1$ of Flory–Huggins theory are observed, while for $|t| \ll$ Gi the Ising-like critical exponents are expected $\{\beta = 0.325, \upsilon_I = 0.63, \gamma = 1.24$ [39]$\}$. One can describe this crossover in terms of a crossover scaling description [7]

$$m_{coex} N^{1/2} = \tilde{\tilde{m}}(tN)\,, \tag{11}$$

where the scaling function $\tilde{\tilde{m}}(y)$ behaves as

$$\tilde{\tilde{m}}(y \ll 1) \propto y^{\beta}, \quad \tilde{\tilde{m}}(y \gg 1) \propto y^{1/2}, \tag{12}$$

to reproduce the correct critical exponents in the regimes $|t| \ll$ Gi and $|t| \gg$ Gi. From Eqs. (11, 12), one immediately sees that the critical amplitude $\hat{B}(N)$ in the Ising-like regime scales as

$$\hat{B}(N) \propto N^{\beta - 1/2} \approx N^{-0.175},$$

Ising-regime, dense melts. (13)

In the mean field regime, of course, $\hat{B}(N)$ is independent of N [1, 42].
Similarly, for the correlation length one can write [44]

$$\xi/N = \tilde{\tilde{\xi}}(tN), \tag{14}$$

where the scaling function $\tilde{\tilde{\xi}}(x)$ behaves as

$$\tilde{\tilde{\xi}}(y \ll 1) \propto y^{-\upsilon_I}, \quad \tilde{\tilde{\xi}}(y \gg 1) \propto y^{-1/2}, \tag{15}$$

and hence the critical amplitudes $\hat{\xi}_{\pm}(N)$ in the Ising-like regime scales are

$$\hat{\xi}_{\pm}(N) \propto N^{1-\upsilon_I} \approx N^{0.37},$$

Ising regime, dense melts. (16)

In the mean-field regime, one has $\hat{\xi}_{\pm}(N) \propto N^{1/2}$, of course [42].
Finally, the collective scattering intensity is written

$$S_{coll}(q \to 0)/N^2 = \tilde{\tilde{S}}(tN), \tag{17}$$

where the scaling function $\tilde{\tilde{S}}(y)$ behaves as

$$\tilde{\tilde{S}}(y \ll 1) \propto y^{-\gamma}, \quad \tilde{\tilde{S}}(y \gg 1) \propto y^{-1}, \tag{18}$$

and hence the critical amplitudes $\hat{\Gamma}_I$ in the Ising critical regime $\{\hat{S}_{coll} = \hat{\Gamma}_I |t|^{-\gamma}\}$ scale as

$$\hat{\Gamma}_{\pm}(N) \propto N^{2-\gamma} = N^{0.76},$$

Ising regime, dense melts, (19)

while in the mean-field regime one has $\hat{\Gamma}_{\pm}(N) \propto N$. These relations have been verified both by recent simulations [44] and experiments [45, 46], and also some of the above crossover scaling functions, $\tilde{\tilde{m}}$, $\tilde{\tilde{S}}$ have been estimated [44–47].

Now, we follow Broseta et al. [18] discussing how this crossover scaling picture has to be modified in the semidilute regime near the overlap concentration ϕ^*. First, one notes that at the (mean-field) critical point the volume fraction ϕ_{crit} taken by monomers can be written as (using Eq. (3))

$$\phi_{crit} \propto [N \varepsilon_{AB}/k_B T_c]^{-(3\upsilon - 1)/(1 + x)}\,. \tag{20}$$

Equation (20) should hold at the actual critical temperature as well (only the constant of proportionality which have been suppressed, differs between the mean-field T_c and the actual T_c, after χ_{eff} is rescaled and N is rescaled as done in Eqs.(2), (3)). Noting that $\phi^* \propto N^{-(3\upsilon - 1)}$, we notice that

$$\phi_{crit}/\phi^* \propto N^{x(3\upsilon - 1)/(1 + x)} (\varepsilon_{AB}/k_B T_c)^{-(3\upsilon - 1)/(1 + x)}\,. \tag{21}$$

Broseta et al. then argue that $\tilde{N}_{crit} \propto (\phi_{crit}/\phi^*)^{1/(3\upsilon - 1)} \propto N^{x/1 + x}$ is the number of blobs per chain at the unmixing critical point, and that it is this number rather than N that one should use in the Ginzburg criterion. Thus, Eq. (11) is replaced by

$$m_{coex} \tilde{N}_{crit}^{1/2} = \tilde{\tilde{m}}(t\tilde{N})\,,$$
$$m_{coex} N^{x/[2(1 + x)]} = \tilde{\tilde{m}}(tN^{x/(1 + x)})\,. \tag{22}$$

Figure 10 shows that the scaling form Eq. (22) is in excellent agreement with our data, while Eq. (11) would not work; similarly, one proceeds for the other quantities as well:

$$\xi/N^{\upsilon_I + x/[2(1 + x)]} = \tilde{\tilde{\xi}}[tN^{x/(1 + x)}]\,, \tag{23}$$

$$S_{coll}(q \to 0)/N^{(2 + x)(1 + x)} = \tilde{\tilde{S}}[tN^{x/(1 + x)}]\,. \tag{24}$$

The asymptotic behavior of the various scaling functions defined in Eqs. (22), (23) and (24) is the same as that in Eqs. (12), (15) and (18), of course; note that prefactors of order unity were suppressed throughout. Thus, one now predicts the

following N-dependence of the critical amplitudes in the Ising regime for blends in semidilute solution [18]

$$\hat{B}(N) \propto N^{x(\beta-1/2)/(1+x)}, \quad \hat{\Gamma}_{\pm} \propto N^{1+x(1-\gamma)/(1+x)}, \quad \hat{\xi}_{\pm} \propto N^{(\upsilon-\upsilon_i x+x)/(1+x)} \tag{25}$$

Taking the Ising values of critical exponents [39] and $x = 0.22$, this yields $\hat{B}(N) \propto N^{0.032}$, $\hat{\Gamma}_{\pm}(N) \propto N^{0.956}$, and $\hat{\xi}_{\pm}(N) \propto N^{0.55}$. The results for $\hat{B}(N)$ and $\hat{\Gamma}_{\pm}(N)$ are in excellent agreement with estimates obtained in early Monte Carlo work on short chains in rather dense systems ($\phi_v = 0.2$) [7].

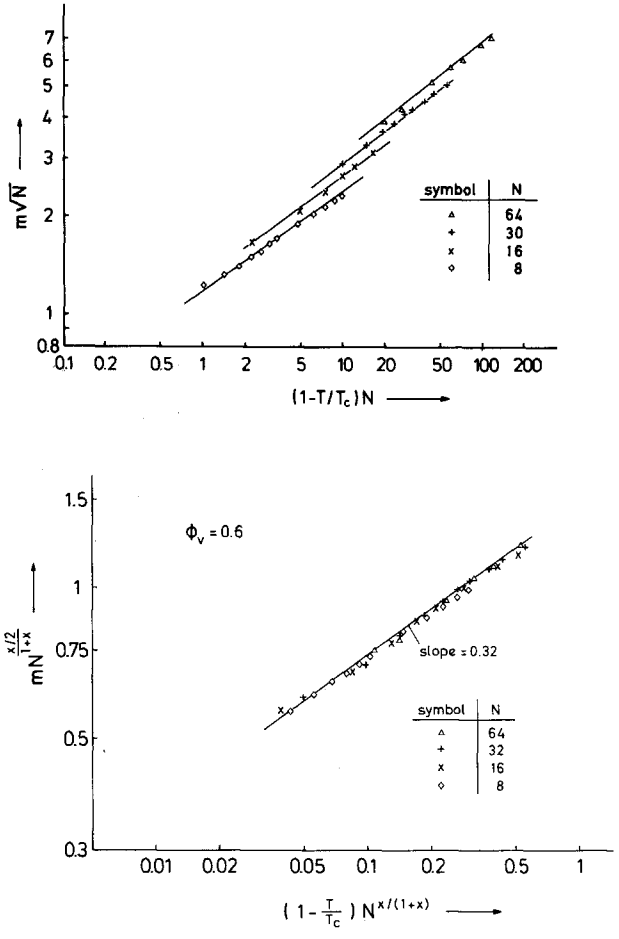

Fig. 10. Data for the order parameter m_{coex} for $\phi_V = 0.6$, $N = 8,16,32$ and 64 plotted in scaling form for dense melts $\{m\sqrt{N}$ vs. $(1 - T/T_c)N$, part $(a)\}$ and in scaling form for semidilute solutions $\{mN^{(x/2)/(1+x)}$ vs. $(1 - T/T_c)\ N^{x/(1+x)}$, part (b)$\}$

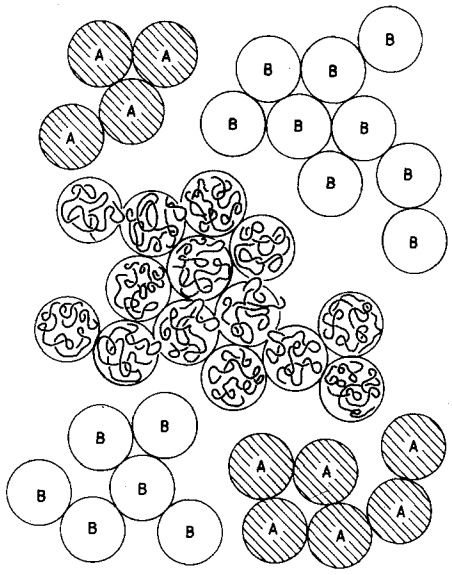

Fig. 11. Schematic picture of coil configurations in the dilute regime for ϕ slightly less than ϕ^*. Coils form clusters that touch each other in their surface region. As $T \to 0$, each cluster is either formed purely by A-chains or by B-chains

5. Concluding remarks

In this study we have investigated the unmixing of binary symmetric polymer blends ($N_A = N_B = N$) in semidilute solutions at volume fractions ϕ near the overlap volume fraction $\phi^* \propto N^{-1/(3\upsilon-1)}$ separating the semidilute regime from the dilute regime. Our Monte Carlo data show that for $\phi \gtrsim \phi^*$ an unmixing transition occurs of the same type as in much denser polymer blends, characterized by Ising-type critcal behavior near T_c, and by complete phase separation between A and B for $T \ll T_c$. The critical temperature scales with volume fraction ϕ and chain-length as predicted in Eq.(3) [17–19], see Fig. 9. The thermodynamic functions $\{m_{coex}$, $S_{coll}(q \to 0)$, the specific heat, Fig. 4$\}$ are very similar to their counterparts in dense systems, and near the critical points we find evidence for the crossover scaling description proposed by Broseta et al. [18] (Fig. 10).

For systems at volume fractions ϕ deep in the dilute regime, however, the unmixing phase transition no longer occurs (Fig. 6). The strong finite size effects that are still present, however,

prove the existence of a large correlation length of volume fraction fluctuations at very low temperatures in that regime. One can interpret this observation in terms of large clusters of coils of the same type, as schematically sketched in Fig. 11. Of course, these clusters are no rigid objects, but due to the random diffusion and conformational rearrangements of the coils these clusters form and decay again, but in spite of this dynamical rearrangement of the cluster pattern, we expect that there is a well-defined mean cluster size, which is essentially controlled by the volume fraction ϕ only. At very low temperatures, this cluster size becomes identical to the correlation length of volume fraction fluctuations (Fig. 11). As ϕ increases, one reaches a percolation threshold $\phi_p < \phi^*$, where for the first time an infinite cluster of coils touching each other becomes possible, spanning in a macroscopic system from one boundary to the other. We argue that a nonzero T_c does exist already for $\phi_p < \phi < \phi^*$, but since the "percolation probability" is less than unity (i.e., not all coils are part of this percolating cluster, some of them form small clusters disjunct from the spanning cluster), the order parameter of the unmixing transition does not saturate as $T \to 0$, and there remain anomalously enhanced volume fraction fluctuations in this limit. Our results for $\phi = 0.15$, $N = 32$ are a rather clear hint towards such a behavior (Fig. 7).

In this regime $\phi_p < \phi < \phi^*$, each coil takes a volume $4\pi\langle R_{gyr}^2\rangle^{3/2}/3 \propto N^{3\nu}$, i.e., the density inside such a coil is of order $N^{1-3\nu}$. Contacts between different coils are possible at the surface area of such coils only. Assuming that the number of such contacts is proportional to the surface area ($\propto \langle R_{gyr}^2\rangle \propto N^{2\nu}$) and to the square of the density inside coils, one would obtain $n_{con} \propto (N^{1-3\nu})^2 N^{2\nu} = N^{2-4\nu}$. Since this exponent is slightly negative, the number of contacts between two neighboring coils can only be of order unity for large N, and hence phase separation now is expected only if $\varepsilon_{AB}/k_B T \gtrsim 1$. This is consistent with our findings (cf. Figs. 5, 7) and is very different from dense melts where phase separation already occurs if $\varepsilon_{AB}/k_B T \gtrsim N^{-1}$.

References

1. For a recent review, see Binder K (1994) Advances Polymer Sci 112:181
2. Walsh DS, Higgins JS, Maconnachie A (eds) (1985) Polymer blends and mixtures. Martinus Nijhoff, Dordrecht
3. Koningsveld R, Kleintjens LA, Nies E (1987) Croat Chim Acta 60:53
4. Binder K (1987) Colloid Polym Sci 265:273; (1988) Colloid Polym Sci 266:871
5. Nose T (1987) Phase Transitions 8:245
6. Hashimoto T (1988) Phase Transitions 12:47
7. Sariban A, Binder K (1987) J Chem Phys 86:5859
8. Sariban A, Binder K (1988) Macromolecules 21:711
9. Schweizer KS, Curro JG (1990) Chem Phys 149:105
10. Yethiraj A, Schweizer KS (1992) J Chem Phys 97:5927; (1993) J Chem Phys 98:9080
11. Schweizer KS, Yethiraj A (1993) J Chem Phys 98:9053
12. Hashimoto T (1993) In: Thomas EL (ed) Materials Science and Technology, Vol. 12, Structure and Properties of Polymers.
13. Lipson JEG (1991) Macromolecules 24:1334
14. Dudowicz J, Freed KF (1991) Macromolecules 24:5076,5112
15. Fredrickson GH and Liu (preprint)
16. Joanny JF, Leibler L, Ball R (1984) J Chem Phys 81:4640
17. Schäfer L, Kappeler Ch (1985) J Phys (France) 46:1853
18. Broseta D, Leibler L, Joanny JF (1987) Macromolecules 20:1935
19. Onuki A, Hashimoto T (1989) Macromolecules 22:879
20. Schäfer L, Kappeler Ch (1990) Colloid Polym Sci 268:995
21. Schäfer L, Kappeler Ch, Lehr U (1991) J Phys (France) II:211
22. Schäfer L, Kappeler Ch (1993) (preprint)
23. Flory PJ (1953) Principles of Polymer Chemistry. Cornell University Press: Ithaca
24. Huggins ML (1941) J Chem Phys 9:440
25. Flory PJ (1941) J Chem Phys 9:660
26. De Gennes PG (1979) Scaling concepts in polymer physics. Cornell University Press: Ithaca
27. Nose T (1986) J Phys (France) 47:517
28. Sariban A, Binder K (1988) Colloid Polym Sci. 266:389
29. Scott RL (1949) J Chem Phys 17:279
30. Shinozaki K, Saito Y, Nose T (1982) Polymer 23:1937
31. Van den Esker M, Vrij A (1976) J Polym Phys Ed 14:1943
32. Fukuda T, Nagata M, Inagaki H (1984) Macromolecules 17:548
33. Nagata M, Fukuda T, Inagaki H (1987) Macromolecules 20:2173
34. For a brief previous account of this point see Binder K (1988) In: Landau DP, Mon KK, Schüttler H-B (eds) Computer Simulation Studies in Condensed Matter Physics (Springer Proceedings in Condensed Matter Physics). Springer, Berlin, p. 84
35. Rosenbluth MN, Rosenbluth AW (1955) J Chem Phys 23:256
36. Kremer K, Binder K (1988) Computer Phys Rep 7:259
37. Deutsch H-P, Binder K (1992) Macromolecules 25:6214
38. For a recent review see Binder K (1992) In: Gausterer A, Lang CB (eds) Computational methods in field theory. Springer, Berlin, p. 59
39. Le Guillou JC, Zinn-Justin J (1980) Phys Rev 1321:3976
40. De Gennes PG (1977) J Phys Lett (Paris) 38:L441

41. Joanny JF (1978)J Phys A11:L117
42. Binder K (1983) J Chem Phys 79:6387
43. Ginzburg VL (1960) Sov Phys Solid State 2:1824
44. Deutsch HP, Binder K (1993) J Phys (Paris) II3:1049
45. Meier G, Schwahn D, Mortensen K, Janßen S (1993) Europhys Lett 22:577
46. Schwahn D, Meier G, Mortensen K, Janßen S (1994) J Phys (Paris) II4, in press
47. Anisimov MA, Kiselev SB, Sengers VJ, Tang S (1992) Physica A188:487

Received April 21, 1994;
accepted June 9, 1994

Authors' address:

Dr. Kurt Binder
Institut für Physik
Johannes-Gutenberg-Universität Mainz
Staudinger Weg 7
55099 Mainz